Prediction of spiral-tip trajectories via pseudo-ECGs and LSTM networks

Vasanth Kumar Babu[1], Jaya Kumar Alageshan[1], Rahul Pandit[1]
[1] Centre for Condensed Matter Theory, Department of Physics, Indian Institute of Science, Bangalore, India

Abstract

Spiral waves of electrical activation in cardiac tissue can lead to life-threatening ventricular arrhythmias. The tracking of the tip of a spiral wave is a problem of central importance that can play an essential role in eliminating these arrhythmias via methods such as catheter ablation. We first obtain pseudo-ECGs from our simulations of spiral waves in the two-dimensional, two-variable Aliev-Panfilov model for cardiac tissue. We then use these pseudo ECGs in conjunction with Long-Short-Term-Memory (LSTM) networks to track the tip trajectories of spiral waves. We demonstrate that our LSTM-based tip-tracking compares favorably with the Iyer-Gray method, which requires the full spatiotemporal evolution of spiral waves to obtain tip trajectories. Our tip-trajectory data include rigid, meandering, and drifting spiral waves. We use the Iyer-Gray method to get the spiral wave trajectories during training and testing. We demonstrate that training with noise can lead to better results in testing data with noise. By using an ensemble of 5 LSTM networks, we show that the number of outliers, in the presence of noise, can be decreased.

1. Introduction

Sudden cardiac death, the primary cause of death in the modern world, is often precipitated by the formation of spiral- or scroll-wave patterns of electrical excitations in ventricular tissue [1]. Therefore, many experimental and numerical studies have been performed to understand, detect, and eliminate such waves [2–5]. Some spiral-elimination methods, e.g., catheter ablation, require the position of the tip (or rotor center) of the spiral wave [4, 5]. Several noninvasive methods have been developed for such tip tracking, for instance, ones that use Electrocardiograms (ECGs) [4, 6, 7] and others that use machine learning with ECGs [8, 9] or with data from *in vitro* experiments or *in silico* investigations of mathematical models for ventricular tissue [10, 11].

Recurrent Neural Networks (RNNs) have been used widely for time-series-based predictions. In particular, RNNs have been employed with ECGs to classify cardiac arrhythmias [see, e.g., Refs. [12, 13]]. We show that Long-Short-Term-Memory (LSTM) networks [14], developed to address some shortcomings of earlier RNNs, can help in tracking the tip trajectories of spiral waves if trained with pseudo-ECGs. We use a vanilla LSTM network for such tracking with pseudo-ECGs from our *in silico* study of the Aliev-Panfilov model [15] for ventricular tissue.

2. Model and Methods

2.1. Aliev-Panfilov model

We obtain spiral waves in the Aliev-Panfilov model [15], a two-variable partial differential equation (PDE) with a fast variable u and a slow variable v.

$$\begin{aligned}\frac{\partial u}{\partial t} &= ku(1-u)(u-a) - uv + D\Delta u;\\ \frac{\partial v}{\partial t} &= (\epsilon + \frac{m_1 v}{m_2 + u})(-v - ku[u-(b+1)]). \quad (1)\end{aligned}$$

u models the behavior of the transmembrane potential and v the averaged effects of ion channels; a, b, m_1, m_2, k, and ϵ are parameters, Δ is the Laplacian, and D is the diffusivity. We use Neumann boundary conditions on a square domain with 128^2 grid points; and we solve these PDEs by using the forward-Euler method for time-marching, a 5-point stencil for the spatial Laplacian, a time step $dt = 0.07$, and a space step $dx = 0.6$ [in dimensionless units that correspond to 0.28ms and 0.6mm [16], i.e., a $76.8 \times 76.8\text{mm}^2$ domain].

2.2. Pseudo ECG

We calculate the Pseudo-ECGs [17] at time t

$$ECG(t) = \sum_i \frac{\delta u_i(t).d^2.cos(\theta_i)}{4\pi.{R_i}^2}, \quad (2)$$

where R_i is the distance between the current dipole at location i and the position of lead where the ECG is measured, δu is the voltage difference between the transmembrane potentials of the neighboring cells, d is the distance between cells, θ_i is the angle between the current dipole at location i and the vector joining it to the lead position, and the summation is over the entire domain.

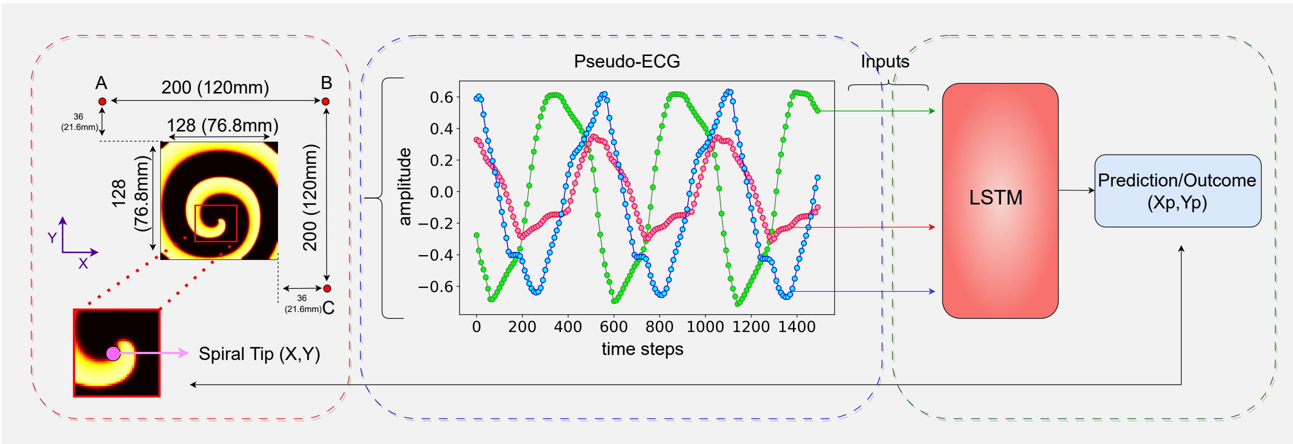

Figure 1. Left panel: Pseudocolor plots of u showing a spiral wave in our *in silico* study of the two-dimensional (2D) Aliev-Panfilov model (1) and the 3 representative locations, A, B, and C, at which we calculate the pseudo-ECGs 2. Middle panel: Pseudo-ECGs (red, blue, and green lines; normalized) from A, B, and C arising from spiral waves in Eq. (1). Right panel: Our LSTM neural network, whose inputs are the pseudo-ECGs and the outputs are spiral-center locations (Xp, Yp).

2.3. Data generation and processing

We use the Aliev-Panfilov model with the parameters of Ref. [18], i.e., $k = 8.0$, $b = 0.1$, $\epsilon = 0.01$, $m1 = 0.2$, $m2 = 1.3$, and $a \in [0.1, 0.2]$, which allow us to obtain rigidly rotating or meandering spirals. Spatial gradients in a lead to drifting spirals. We use $a(x,y) = a_0 + (\partial a(x,y)/\partial x) * x + (\partial a(x,y)/\partial y) * y$; for a given spiral trajectory, a_0 and these partial derivatives are fixed; but they are chosen (uniformly) randomly to generate different spiral trajectories such that $a(x,y) \in [0.1, 0.2]$. We initiate the spirals with broken-wavefront initial conditions. We re-scale our pseudo-ECG and spiral-tip positions such that they lie in the range $[-1, 1]$ before we feed them into the LSTM network.

2.4. Spiral-tip tracking: Iyer-Gray method

We use the Iyer-Gray method [11] to track the spiral tip. We calculate the phase

$$\theta \quad = \quad \tan^{-1}\left(\frac{u(t+\tau) - u_m}{u(t) - u_m}\right), \tag{3}$$

where $u(t)$, $u(t+\tau)$, and u_m represent, respectively, the voltage at times t, $t+\tau$ and the mean voltage. The points around which the condition

$$\oint \nabla\theta . dr = \pm 2\pi \tag{4}$$

is satisfied yield the locations of spiral tips.

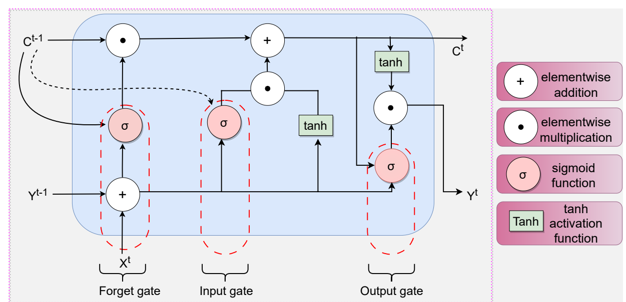

Figure 2. Schematic diagram of our LSTM network, with X^t the input at time t, and C^t and C^{t-1} cell states at t and $t-1$, respectively, Y^t, Y^{t-1} is the output at t and $t-1$.

2.5. Long short term memory network

The schematic diagram of our vanilla LSTM block [Fig. 2] shows its 4 main components: cell, and forget, input, and output gates. The LSTM cell state [C^t in Fig. 2] leads to a *gradient highway* along which information can propagate over a large sequence of input data; this circumvents the vanishing-gradient problem [14]. Y^t and Y^{t-1} in Fig. 2 are the outputs of the LSTM at time steps t and $t-1$; and X^t is the input. For LSTM, we use Tensorflow [19].

3. Results

We consider rigidly rotating spirals that have small cores, meandering spirals with larger cores, and drifting spirals. We use 20000 trajectories (1000 points each) for training. In Fig. 3 (a), we show some test trajectories (1000 points each), of the 5000 we employ for testing. We

SNR dB	D_p [Trained: no noise]	D_p [Trained: SNR 5dB]
∞	1.26 ± 0.60 [0.76mm $\pm$ 0.36mm]	4.46 ± 3.86 [2.68mm $\pm$ 2.31mm]
30	4.80 ± 3.67 [2.88mm $\pm$ 2.20mm]	5.05 ± 4.36 [3.03mm $\pm$ 2.61mm]
25	10.52 ± 7.14 [6.31mm $\pm$ 4.28mm]	5.08 ± 4.38 [3.05mm $\pm$ 2.63mm]
20	17.89 ± 10.68 [10.73mm $\pm$ 6.41mm]	5.14 ± 4.38 [3.08mm $\pm$ 2.63mm]
15	26.08 ± 13.15 [15.65mm $\pm$ 7.89mm]	5.30 ± 4.42 [3.18mm $\pm$ 2.65mm]
10	39.06 ± 16.63 [23.44mm $\pm$ 9.98mm]	6.02 ± 4.69 [3.61mm $\pm$ 2.81mm]
5	52.58 ± 20.98 [31.55mm $\pm$ 12.59mm]	8.72 ± 5.65 [5.23mm $\pm$ 3.39mm]

Table 1. D_ps [Eq. (5)] for LSTMs trained without noise [column 2] and with SNR = 5 dB [column 3] and tested on data with noise [column 1]; D_p is in grid points and dimensioned units [in square brackets].

store the pseudo-ECG and tip locations every 10 steps; the pseudo-ECG time series [length 50] is the input, and the spiral-tip location at the final time is the output. We use single-layer LSTMs [512 nodes each], train them for 40 epochs, and use the root-mean-square loss function and the L_2 regularizer.

$$D_p \equiv \sqrt{\langle (X - X_p)^2 + (Y - Y_p)^2 \rangle}\,, \tag{5}$$

measures the average deviation of the spiral tip (Xp, Yp), predicted by our LSTM, from the Iyer-Gray prediction (X, Y), for a given trajectory ($\langle \cdot \rangle$ is the average over a trajectory). We present our results for 5000 trajectories in Table 1: column 2 is for data with no noise in training and testing with varying noise. To study the effects of Gaussian noise, we calculate the signal-to-noise ratio [20]

$$\text{SNR} \equiv 10 \log_{10} \left[\frac{\sum_t \left(ECG'(t)\right)^2}{\sum_t \left(ECG(t) - ECG'(t)\right)^2} \right], \tag{6}$$

where $ECG(t)$ and $ECG'(t)$ are the pseudo-ECG with and without noise. We train our LSTMs with SNR 5dB data, test them on SNR 30, 25, 20, 15, 10 , and 5 dB, and give our results in Table 1: column 3, which shows the improvement in performance with noise-trained LSTMs.

We define outliers as the points whose predictions have deviations $\geq 3D_p$. When training and testing our LSTMs without noise, $\simeq 0.4\%$ of our data show outliers. The percentage of outliers increases with the noise level: when training and testing with SNR = 5 dB, the outlier percentage $\simeq 2.69\%$, which we can reduce by using an ensemble of LSTM networks as follows. We train 5 LSTM networks independently, with SNR = 5 dB; and we obtain the final prediction by averaging over these 5 networks; this reduces the outlier percentage to $\simeq$ 1.46% [Fig 3: right panel]: The closer the predictions are to the mean, the fewer the outliers.

4. Conclusions

We develop an LSTM-based tracking method for the tip-tracking method for spiral waves in the Aliev-Panfilov model (1). Our LSTM-based tip-tracking compares favorably with the Iyer-Gray method, which requires the full spatiotemporal evolution of spiral waves; e.g., we use LSTM predictions with the inputs of size 150 [50 points from 3 leads], whereas the Iyer-Grey method requires information from $16834 = 128^2$ grid points. We use the Iyer-Gray method to get the spiral wave trajectories during the training and testing of our LSTMs. We demonstrate that training with noise can improve results in testing data with noise. By using an ensemble of 5 LSTM networks, we show that the number of outliers, in the presence of noise, can be decreased. It would be useful to extend our LSTM-based tip-tracking method to spiral waves in biophysically realistic mathematical models for cardiac tissue.

Acknowledgments

We thank SERB and the National Supercomputing Mission (India) for support and SERC (IISc) for computational resources.

References

[1] Jalife J. Rotors and Spiral Waves in atrial fibrillation. Journal of Cardiovascular Electrophysiology 2003;14(7):776–780.

[2] Shajahan T, Nayak AR, Pandit R. Spiral-Wave Turbulence and its Control in the Presence of Inhomogeneities in Four Mathematical Models of Cardiac Tissue. PLOS ONE 2009; 4(3):e4738.

[3] Pandit SV, Jalife J. Rotors and the Dynamics of Cardiac Fibrillation. Circulation research 2013;112(5):849–862.

[4] Rappel WJ, Zaman JA, Narayan SM. Mechanisms for the Termination of Atrial Fibrillation by Localized Ablation: Computational and Clinical studies. Circulation Arrhythmia and Electrophysiology 2015;8(6):1325–1333.

[5] Sommer P, et al. Successful Repeat Catheter Ablation of Recurrent Longstanding Persistent Atrial Fibrillation with Rotor Elimination as the Procedural Endpoint: A Case series. Journal of Cardiovascular Electrophysiology 2016; 27(3):274–280.

[6] Luongo G, et al. Non-Invasive Identification of Atrial Fibrillation Driver Location Using the 12-lead ECG: Pulmonary Vein Rotors vs. other Locations. In 2020 42nd Annual International Conference of the IEEE Engineering in

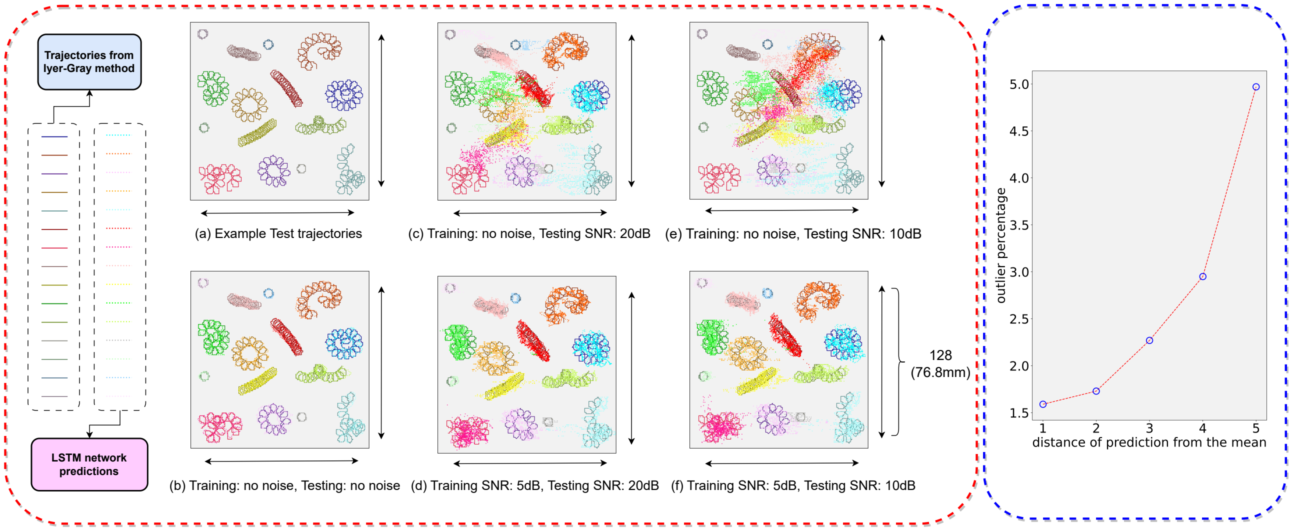

Figure 3. Left panel: (a) illustrative test trajectories; (b) LSTM predictions [trained and tested without noise] for these trajectories; (c) and (d): predictions for the cases where the LSTM is trained without noise and with noise [SNR = 5 dB] and tested on SNR = 20 dB. (e) and (f): as in (c) and (d) but for tested with SNR = 10 dB. Note that predictions are improved significantly by training with noise. Right panel: Plot of the number of outliers (see text) versus the distance of the predictions from the mean. [We train 5 LSTM networks independently, with SNR = 5 dB; we obtain the final prediction by averaging over these 5 networks (and order these predictions in increasing order of their distance from the mean (1-5)); this reduces the outlier percentage to $\simeq 1.46\%$. The closer the predictions are to the mean, the fewer the outliers.]

Medicine & Biology Society (EMBC). IEEE, 2020; 410–413.

[7] Rodrigo M, et al. Body surface localization of left and right atrial high-frequency rotors in atrial fibrillation patients: A clinical-computational study. Heart Rhythm 2014; 11(9):1584–1591.

[8] Yang T, et al. Localization of Origins of Premature Ventricular Contraction by Means of Convolutional Neural Network from 12-lead ECG. IEEE Transactions on Biomedical Engineering 2017;65(7):1662–1671.

[9] Monaci S, et al. Automated Localization of Focal Ventricular Tachycardia From Simulated Implanted Device Electrograms: A Combined Physics–AI Approach. Frontiers in Physiology 2021;12.

[10] Fenton F, Karma A. Vortex dynamics in three-dimensional continuous myocardium with fiber rotation: Filament instability and fibrillation. Chaos An Interdisciplinary Journal of Nonlinear Science 1998;8(1):20–47.

[11] Iyer AN, Gray RA. An Experimentalist's Approach to Accurate Localization of Phase Singularities during Reentry. Annals of Biomedical Engineering 2001;29:47–59.

[12] Singh S, Pandey SK, Pawar U, Janghel RR. Classification of ECG Arrhythmia using Recurrent Neural Networks. Procedia Computer Science 2018;132:1290–1297.

[13] Saadatnejad S, Oveisi M, Hashemi M. LSTM-based ECG Classification for Continuous Monitoring on Personal Wearable Devices. IEEE Journal of Biomedical and Health Informatics 2019;24(2):515–523.

[14] Hochreiter S, Schmidhuber J. Long Short-term memory. Neural Computation 1997;9(8):1735–1780.

[15] Aliev RR, Panfilov AV. A simple two-variable model of cardiac excitation. Chaos Solitons Fractals 1996;7(3):293–301. ISSN 0960-0779.

[16] Panfilov AV, others. Elimination of spiral waves in cardiac tissue by multiple electrical shocks. Phys Rev E Apr 2000; 61:4644–4647. URL `https://link.aps.org/doi/10.1103/PhysRevE.61.4644`.

[17] Virag N, Vesin JM, Kappenberger L. Electrocardiogram simulation with an ionic current computer model of the cardiac tissue. Engineering in Medicine and Biology Society Vol20 Proceedings of the 20th Annual International Conference of the IEEE 1998;32–35 vol.1.

[18] Rusakov A, Medvinsky AB, Panfilov AV. Scroll waves meandering in a model of an excitable medium. Phys Rev E Aug 2005;72:022902.

[19] Abadi M, et al. Tensorflow: A System for Large-Scale Machine Learning. In 12th {USENIX} Symposium on Operating Systems Design and Implementation ({OSDI} 16). 2016; 265–283.

[20] Samann F, Schanze T. An efficient ECG Denoising method using Discrete Wavelet with Savitzky-Golay filter. Current Directions in Biomedical Engineering 2019;5(1):385–387.

Address for correspondence:

Vasanth Kumar Babu
Department of Physics, IISc, Bangalore-560012, India
vasanthkumarb42@gmail.com,vasanthb@iisc.ac.in